Design of an interventional magnetic resonance imaging coil for cerebral surgery

Xu Yue(许 跃), Wang Wen-Tao(王文韬), and Wang Wei-Min(王为民)†

Institute of Quantum Electronics, School of Electronic Engineering and Computer Science, Peking University, Beijing 100871, *China*

(Received 15 March 2012; revised manuscript received 18 May 2012)

In clinical magnetic resonance imaging (MRI), the design of the radiofrequency (RF) coil is very important. For certain applications, the appropriate coil can produce an improved image quality. However, it is difficult to achieve a uniform B1 field and a high signal-to-noise ratio (SNR) simultaneously. In this article, we design an interventional transmitter-and-receiver RF coil for cerebral surgery. This coil adopts a disassembly structure that can be assembled and disassembled repeatedly on the cerebral surgery gantry to reduce the amount of interference from the MRI during surgery. The simulation results and the imaging experiments demonstrate that this coil can produce a uniform RF field, a high SNR, and a large imaging range to meet the requirements of the cerebral surgery.

Keywords: magnetic resonance imaging, Maxwell equation, uniformity, signal-to-noise ratio

PACS: 87.61.–c, 87.61.Ff, 84.32.Hh **DOI:** 10.1088/1674-1056/21/11/118704

1. Introduction

Since the beginning of the 1980s, magnetic resonance imaging (MRI) has been established as a promising diagnostic tool.[1] Over the past 30 years, the application of MRI techniques in clinical research has been significantly developed and has increased in number. The MRI has significant advantages. For example, it is free of ionizing radiation, provides relatively good spatial and temporal resolutions, has a better soft tissue contrast than CT and X-rays, and has high intrinsic contrasts for various types of tissues, which can produce a high-quality image without using a contrast agent.[1] The disadvantages of the MRI include the safety aspects of the MRI environment. When designing magnetic resonance (MR) facilities and choosing the patient monitoring instruments, the magnetic field must be taken into account. Most standard surgical instruments cannot be used in a strong magnetic field, and all of the equipment and instruments used in the MRI must be MR-compatible and MR-safe.[2,3]

The MRI can be divided into the whole-body MRI and the mini MRI based on the imaging range. The whole-body MRI is widely used because it can scan multiple parts of the body. However, the whole-body MRI has several disadvantages, for example, it takes up a lot of space, so it is difficult to use in a conventional operating room.[4] Compared with the whole-body MRI, the mini MRI scans fewer parts of the body but uses equipment that is smaller and is more convenient for use in a surgery room.

The MRI image quality is affected by many factors, among which the performance of the imaging coil is the most important. The common MRI imaging coils include surface coils, birdcage coils, and phased array coils. Different types of coils are used for different purposes. A suitable coil for practical application should balance the signal-to-noise ratio (SNR) and the radiofrequency (RF) field uniformity.[5,6] The surface coil offers a high SNR; however, the SNR sharply decreases as the distance increases, and the B1 field is not uniform.[7] Although the birdcage coil[8−10] cannot offer a very high SNR, it is known to provide a highly uniform B1 field, which results in a high image uniformity; thus, the birdcage coil is often used as the transmitting coil.[11] Compared with those coils, the phased array coils can offer a higher SNR, but their B1 field uniformity is not very good.[11] The quartered dual-channel coil can provide a higher SNR than the single-channel receiver coil and is often used in low-field MRI applications.

Cerebral surgery requires the imaging coils to generate a uniform field to cover the brain region. It also requires that the RF power should not be too large

†Corresponding author. E-mail: wmw@pku.edu.cn

© 2012 Chinese Physical Society and IOP Publishing Ltd

to avoid harming the human body. In this article, we describe the process of designing and building an MRI-transmitter-and-receiver RF coil that utilizes a disassembly structure. Simulations and volunteer imaging experiments have been conducted on the newly designed coil.

2. Model and method

2.1. Coil design and construction

To facilitate the surgery and reduce the number of MRI motion artifacts, the head of the patient must be fixed on the gantry of the operation table during surgery. Meanwhile, acquiring repeated MRI scans is essential to monitor the results of the operation, which means that the conventional MRI coils are not suitable for cerebral surgery. We also need to consider two more factors during surgery. One is that the patient's nose often needs to be accessible for life-support equipment, such as a breathing tube, which means that the imaging coil requires extra space near the nose. The other is that the patient's head sometimes needs to be wrapped with gauze, thus, the imaging coil should have a certain amount of axial space allocated for this purpose.

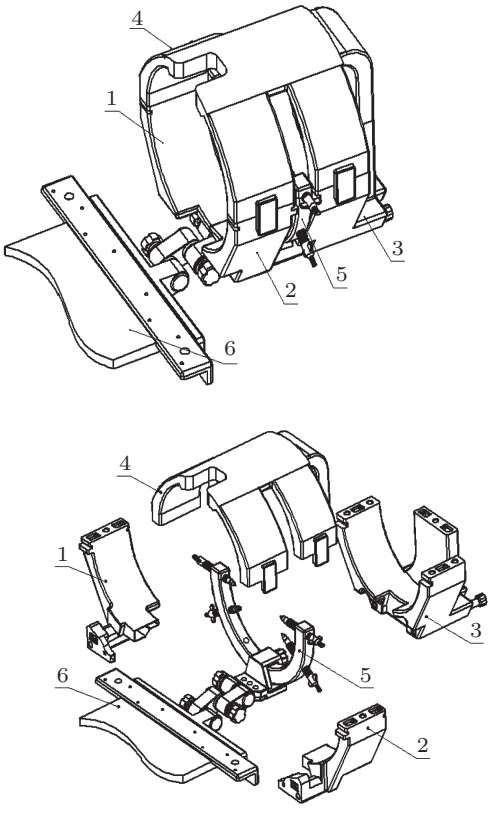


Fig. 1. Cerebral surgery coil structure. Panel (a) shows the imaging coil assembly structure on the surgery gantry; panel (b) is the exploded view of the coil structure. The coil can be split into four components and assembled when necessary. Part 1 is the lower left part of the coil, part 2 is the lower right part of the coil, part 3 is the back of the coil, part 4 is the upper part of the coil, part 5 is the surgery stent, and part 6 is the connection between the operation table and the surgery stent. The operation table is not included in this figure.

Considering all the application characteristics of the cerebral surgery above, we design an RF imaging coil structure as follows. The frame of the coil is composited with a copper band that is 15 mm wide and 0.2 mm thick. This coil uses a dual-channel structure, which has a loop channel and a saddle channel. The space between the loop coils is used to place the surgery gantry. This coil consists of four parts, which can be assembled and disassembled on the surgery gantry repeatedly. There is a hollow area in the front of the coil so the patient's nose can be properly exposed for a more convenient surgery. To obtain a high SNR while maintaining a suitable axial imaging range, the diameter of the coil is initially set to 230 mm, and the axial length is set to 240 mm. However, the aforementioned coil size parameters need to be optimized through a numerical simulation study. Figure 1 shows the imaging coil assembly structure on the gantry and the exploded view of the coil structure.

2.2. Simulation and optimization

To evaluate the performance of the coil, we conduct a numerical simulation to optimize its size. The three-dimensional electromagnetic simulation software ANSYS Ansoft HFSS V12 is used to calculate the electromagnetic field. The calculations are based on Maxwell's time domain equations

$$\nabla \times \boldsymbol{E} = -\frac{\partial \boldsymbol{B}}{\partial t}, \tag{1}$$

$$\nabla \times \boldsymbol{H} = \frac{\partial \boldsymbol{D}}{\partial t} + \sigma_{\mathrm{e}} \boldsymbol{E}, \tag{2}$$

where $\boldsymbol{E}$ ($\mathrm{V \cdot m^{-1}}$) and $\boldsymbol{H}$ ($\mathrm{A \cdot m^{-1}}$) are the electric and the magnetic field intensities, respectively; $\boldsymbol{D}$ ($\mathrm{C \cdot m^{-2}}$) and $\boldsymbol{B}$ ($\mathrm{Wb \cdot m^{-2}}$) are the electric and the magnetic flux densities, respectively; and σ_{e} ($\Omega^{-1} \cdot \mathrm{m^{-1}}$) is the electric conductivity. The above two vector equations in fact represent six scalar equations, one for each of the x, y, and z components of the equations.[12]

Figure 2 is the model of the coil used for the simulation, the structure and the size of which are the same as those of the actual coil. The back of the saddle coil is closed to improve the SNR. We put a 140 mm

(length) × 140 mm (width) × 140 mm (depth) water-filling object at the center of the coil to mimic the human brain. The relative permeability of the filling object is 0.999991, the relative permittivity is 81, and the electric conductivity is 4 S/m. The relative permeability of the copper is 0.999991, the relative permittivity is 1, and the electric conductivity is 58×10^7 S/m.

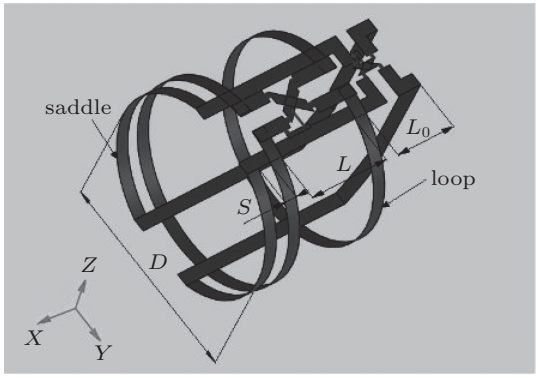


Fig. 2. Simulation model of the coil.

The two most important indicators used to evaluate the performances of the coil are the RF field uniformity and the quality value (Q value) of the coil. A more uniform RF field means that a larger uniform magnetic resonance signal intensity is received and a uniform image can be achieved. The image SNR is closely related to the Q value of the coil. A higher Q value implies a higher SNR of the image. The relationship between the Q value and the SNR is described in the following formula:[13]

$$\mathrm{SNR} \propto \sqrt{\frac{\omega_0 \mu_0 Q}{4kTV_{\mathrm{eff}}\Delta f}}, \tag{3}$$

where ω_0 is the nuclear magnetic resonance (NMR) angular frequency in a static magnetic field, μ_0 is the relative permeability, V_{eff} is the effective volume, and Δf is the 3 db bandwidth of the reflection curve.

We define the RF field uniformity U (i.e., the image uniformity) in an area by the following formula:[11]

$$U = (I_{\max} - I_{\min})/(I_{\max} + I_{\min}), \tag{4}$$

where $I_{\max}$ and $I_{\min}$ are the maximum and the minimum signal intensities within the region of interest (ROI). Thus, a lower value of U corresponds to a higher uniformity within the image. The U value is related to the selection of the ROI. Experiments have been conducted by Kocharian *et al.*[12] on different coils. To calculate U, they chose an area of 45% of the image obtained in the center as the ROI. The results showed that the U values of the body coil and the surface coil were 0.287 and 0.453, respectively, for a good image quality.

Compared with the common MRI head coils, three parameters of this new cerebral surgery coil need to be optimized, they are the coil diameter D, the length of the loop coil along the operation table (labeled as L in Fig. 2), and the spacing between the front of the loop coil and the saddle coil (labeled as S in Fig. 2).

The coil diameter D must match both the human head size and the gantry size. Therefore, D is set to 230 mm for our application. The back of the saddle coil is closed to improve the SNR, and the surgery gantry is fixed between the loop coils; thus, the distance L_0 between the loop coil and the back of the saddle coil should not be too long. For surgical applications, we need to set aside some space on the top of the head for the gauze material, and this distance cannot be too short. Based on these considerations, we set L_0 to 60 mm.

A longer coil length along the axis of the x direction in Fig. 2 is beneficial for cerebral surgeries, but the coil loss increases and the filling factor of the coil decreases as the axial length increases. In the simulations, we change L from 80 mm to 110 mm to explore the Q–L relationship. According to the simulation results, it is more appropriate to make L equal to 100 mm. Figure 3 shows the Q values corresponding to different values of L.

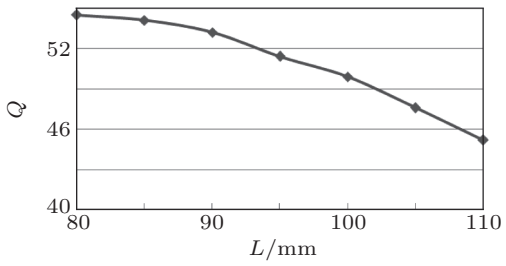


Fig. 3. The Q values corresponding to different values of L.

The spacing S between the front of the loop coil and the saddle coil has a significant influence on the uniform area and needs to be optimized. We change S to obtain a uniform area. We choose a 14 cm × 20 cm rectangular area in the B1 field distribution map as the ROI to calculate the U value. This area is 2 cm away from the back of the coil and encompasses approximately 40% of the total image area. Figure 4 shows the B1 field distributions in the ROI when S equals 15 mm, 30 mm, and 45 mm respectively. Figure 5 shows the U values corresponding to different values of S.

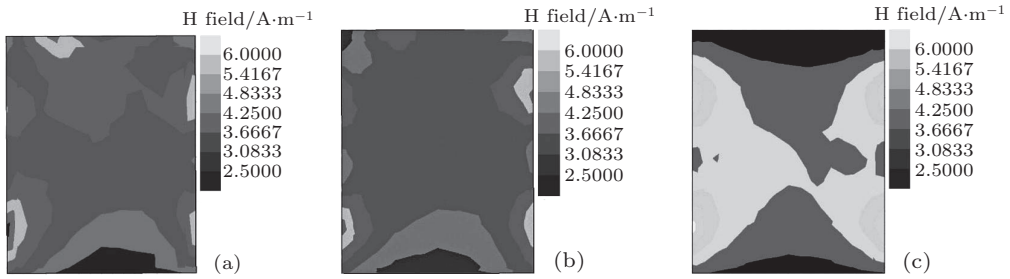


Fig. 4. The B1 field distributions in the ROI when S equals (a) 15 mm, (b) 30 mm, and (c) 45 mm.

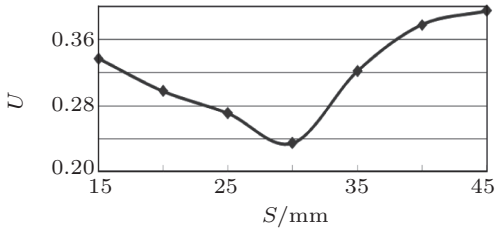


Fig. 5. The U values corresponding to different S.

3. Results and discussion

According to the simulation results, we build an actual cerebral surgery MRI coil. The axial length of the coil is 235 mm, and its diameter is 230 mm. The spacing between the front of the loop coil and the saddle coil S is 30 mm. Figure 6 shows the coil and its application in the cerebral surgery.



Fig. 6. Coil built and its application in cerebral surgery.

To evaluate the performance of the coil, a water phantom was used, and the images were acquired on a 0.23 T MRI scanner. The resonant frequency of the coil was tuned to 9.78 MHz, and the coil was matched to 50 Ω. We used a cubic water phantom doped with $CuSO_4$ and NaCl (the solute concentrations were 1.18 g/L and 5 g/L, respectively) to obtain the image. Two-dimensional images were acquired using a T1-weighted image sequence (matrix size 256 × 256, TR=400 ms, TE=14.5 ms, flip angle=90°, slice thickness=5 mm, FOV=230 mm × 230 mm, number of excitations (NEX)=2). Figure 7 is the water phantom image. The cubic phantom extends over a large proportion of the coil volume. Both the two channels were used for imaging acquisition. We can see that the image is uniform, and no dark area appears in the FOV, indicating that the coil produces a homogeneous RF field.



Fig. 7. Water phantom image.

The SNR is one of the most important measurements of the performance of an MRI system. There are several ways to calculate the SNR from the MRI image. One method that can be used to calculate the SNR requires only one image. The noise is measured in a region drawn over an area of no signal. Three regions are drawn to calculate the SNR, including two small circular regions placed on the background air pixels and a large circular region covering most of the test object. In this method, the SNR is given by[14]

$$\mathrm{SNR}_{\mathrm{single}} = 0.655\frac{S}{S_{\mathrm{Dair}}}, \tag{5}$$

where S is the mean signal in the large circular region, and S_{Dair} is the average of the standard deviation in the two smaller regions.

We use this method to calculate the SNR. The SNR is 36 when only the loop channel is used, 28 when only the saddle channel is used, and 42 when both channels are used. The SNR of the quadratured dual-channel coil is greatly improved compared from that of the single-channel coil.

In addition, we have used this coil to obtain images during a cerebral surgery. The MR parameters to obtain T2-weighted images were as follows: matrix size =256 × 152, TR= 4190 ms, TE=120 ms, flip angle=90°, slice thickness=7 mm, FOV=200 mm × 250 mm, NEX=4.

In total three surgical excisions of a tumor have been conducted consecutively. After each surgical excision, the coil was assembled on the surgery gantry first, then the MRI images were taken, and finally the coil was disassembled for the next surgical excision. Figure 8 shows the T2-weighted images of the patient's head after the first and the second surgical excisions in the same anatomical position. From the images, we can see that the organs are clearly visible, and the images are uniform. No dark area is observed in the imaging region, as the surgeries required. The brain tumor is significantly excised. The surgery results demonstrate that this coil has a good imaging capability to help doctors carry out the surgery.

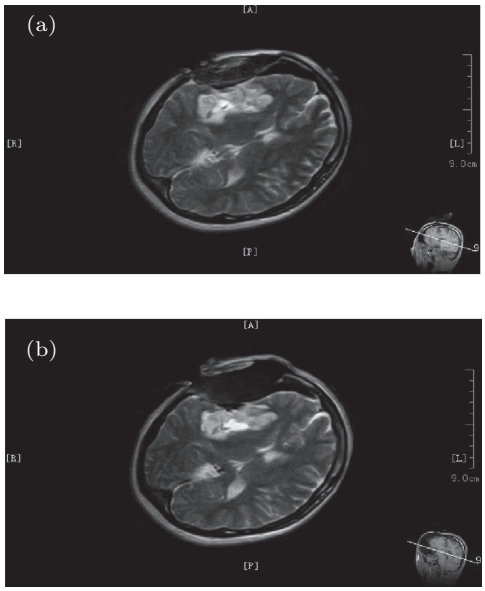


Fig. 8. T2-weighted images obtined after (a) the first and (b) the second surgical excisions.

The non-invasive nature of imaging makes the MRI an ideal tool for diagnosis of human patients. We can simply assess the qualities of the MR images in terms of resolution and contrast. The Q value of a coil and the RF field homogeneity are both very important. However, it is difficult to achieve a high Q value and a uniform B1 field simultaneously. Though we can design the transmitting and receiving coils separately, this increases the complexity of the coils, and we should consider the coupling between the coils.

The newly designed coil adopts a detachable structure that can be assembled and disassembled repeatedly on the cerebral surgery gantry to reduce the amount of interferences from the MRI during surgery, which is among the leading levels in China. The long axial imaging range perfectly meets the requirements of the cerebral surgery. This coil is applied in permanent magnet imaging now. Considering the superconducting imaging applications in the future, we can increase the number of channels based on the structure of the coil to improve the imaging speed, so as to expand the application range of this coil.

4. Conclusion

In this article, we design and build a quadratured dual-channel transmitter-and-receiver MRI RF coil. This coil adopts a disassembly structure to take images multiple times during a cerebral surgery. The coil can generate a uniform B1 field, provide a high SNR, and has a large imaging range. The simulation and the experimental results show that this coil perfectly meets the requirements of cerebral surgery. The RF coil developed in this article has an important reference value for cerebral surgery.

Acknowledgment

The authors are indebted to Dr. Morita and Dr. Ooguro in NTT Medical Center Tokyo for their valuable support in this work.

References

[1] Blanco R T, Ojala R, Kariniemi J, Perälä J, Niinimäki J and Tervonen O 2005 *Eur. J. Radiol.* **56** 130

[2] Jolesz F A and Blumenfeld S M 1994 *Magn. Reson.* Q **10** 85

[3] Lewin J S, Petersilge C A, Hatem S F, Duerk J L, Lenz G, Clampitt M E, Williams M L, Kaczynski K R, Lanzieri C F, Wise A L and Haaga J R 1998 *AJR Am. J. Roentgenol.* **170** 1593

[4] Ladd S C 2007 *C2I2* **4** 8

[5] Radack D M, Schweitzer M E and Taras J 1997 *AJR Am. J. Roentgenol.* **169** 1649

[6] Mondale K, Dai G, Chu A, Burnham R S and Snyder R E 1999 *AJR Am. J. Roentgenol.* **172** 1581

[7] Barberi E A, Gati J S, Rutt B K and Menon R S 2000 *Magn. Reson. Med.* **43** 284

[8] Amari S, Ulug A, Bormemann J, Zijl P and Barker P 1997 *Magn. Reson. Med.* **37** 243

[9] Shen G, Boada F and Thulborn K 1997 *Magn. Reson. Med.* **38** 717

[10] Leifer M 1997 *Magn. Reson. Med.* **38** 726

[11] Kocharian A, Adkins M C, Amrami K K, McGee K P, Rouleau P A, Wenger D E, Ehman R L and Felmlee J P 2002 *Radiology* **223** 870

[12] Kocharian A, Felmlee J P, McGee K P, Riederer S J and Ehman R L 2000 *Magn. Reson. Med.* **44** 660

[13] Zu D L 2004 *Magnetic Resonance Imaging* (1st edn.) (Beijing: Higher Education Press) p. 149 (in Chinese)

[14] Firbank M J, Coulthard A, Harrison R M and E D 1999 *Phys. Med. Biol.* **44** 261